

# Pressure-induced physical changes of noble gases implanted in highly stressed amorphous carbon films

R. G. Lacerda,\* M. C. dos Santos, L. R. Tessler, P. Hammer, F. Alvarez, and F. C. Marques  
*Universidade Estadual de Campinas, Instituto de Física "Gleb Wataghin" 13083-970, Campinas-SP, Brazil*  
 (Received 19 July 2002; revised manuscript received 23 April 2003; published 5 August 2003)

Noble gases (Ar, Kr, and Xe) were trapped in an amorphous carbon matrix in the 1–11-GPa pressure range. Extended and near-edge x-ray-absorption spectroscopies indicate clustering of noble gases induced by the host matrix internal pressure. Simultaneously, the matrix pressure promotes a shift of the noble-gas core-level binding energy of  $\sim 1$  eV. The Auger parameter reveals that both the initial state and the host relaxation terms contribute to the binding-energy shift. *Ab initio* calculations performed on an Ar<sub>7</sub> cluster and on Ar atoms clustered in aromatic molecules support the experimental findings.

DOI: 10.1103/PhysRevB.68.054104

PACS number(s): 61.10.Ht, 36.40.-c, 79.60.-i

## I. INTRODUCTION

Solid noble gases and noble-gas (NG) clusters present intriguing properties and have been the focus of intense experimental and theoretical investigations.<sup>1–4</sup> Their physical properties are extremely sensitive to size,<sup>1–3</sup> temperature,<sup>4</sup> and pressure.<sup>5–7</sup> When implanted in solid matrices, NGs can precipitate in the form of clusters,<sup>6,8–11</sup> however, the clustering kinetics has not yet been established. In the present work, we report detailed investigations of the interactions between noble gases (Ar, Kr, and Xe) and the internal pressure of an amorphous carbon matrix (*a*-C). By intentionally changing the *a*-C deposition conditions, NG atoms were trapped under controlled internal pressures (or intrinsic stress), which could be varied from approximately 1 GPa to 11 GPa. This enables us to investigate the evolution of both electronic and structural properties of clustered NGs as a function of pressure provided by the host matrix. The choice of *a*-C films as a host takes advantage of the well-known stress characteristic of such films, which can achieve very high values. Moreover, the NGs are implanted during the deposition process, without the need for postgrowth ion implantation that can modify the host mechanical properties. This is an alternative and interesting approach for studying noble gases under high pressure, allowing comparison with results of conventional diamond-anvil cells. Auger and photoelectron spectra were applied to study the relationship between the NG core-level energies and the matrix pressure. X-ray appearance near-edge structure (XANES) and extended x-ray-absorption fine structure spectroscopies (EXAFS) were used to probe the local NG environments. Theoretical calculations on model systems at the molecular mechanics level, combined with *ab initio* electronic structure calculations, were also performed to assess the NG interaction with the *a*-C matrix.

## II. EXPERIMENT

Thin *a*-C films were prepared by ion-beam-assisted deposition at 150 °C using Ar, Kr, and Xe gases. The film thicknesses were in the 80–100 nm range. x-ray photoemission spectroscopy (XPS) ultraviolet photoemission spectroscopy (UPS), electron energy-loss spectroscopy (EELS), transmission electron microscopy, and Raman scattering indicate that the material is composed of a compressed and dense *sp*<sup>2</sup>

network (90% by EELS). By carefully controlling the deposition conditions, *sp*<sup>2</sup> rich amorphous carbon films with different internal pressures (or stress, from 1 GPa to about 12 GPa) were prepared. Some 3% residual noble gases (determined by Rutherford backscattering spectroscopy) were trapped in the film during deposition and subjected to the highly strained environment of the *a*-C matrix. Detailed information on the structural properties of these films can be found elsewhere.<sup>12,13</sup> *In situ* photoemission spectroscopy (XPS/UPS, Al *K*α) was used to determine the NG core-level energies [Ar 2*p*, Kr 3*p*(3*d*), and Xe 3*d*(4*d*)]. All measured binding energies of the implanted gases were referenced to the Fermi level by subtracting the work function of the spectrometer. XANES/EXAFS measurements of the Ar *K* edge (3.2 keV), Kr *K* edge (14.3 keV), and Xe *L*<sub>III</sub> edge (4.75 keV) were performed at the Laboratório Nacional de Luz Síncrotron (LNLS) in Campinas, Brazil, using total electron yield (Ar and Xe) or fluorescence (Kr) detection.<sup>14,15</sup> Stress measurements were performed on films deposited on 4 × 25 × 0.4-mm<sup>3</sup> (111) *c*-Si bars, using the bending beam method to determine the radius of curvature of the film/substrate composite. An apparatus based on the deflection of a He-Ne laser was used for that purpose.<sup>16</sup> The stress  $\sigma$  was then calculated using Stoney's equation:<sup>17,18</sup>

$$\sigma = [E/(1 - \nu)](t^2/6d)(1/R - 1/R_0), \quad (1)$$

where  $E = 229$  GPa,  $\nu = 0.262$ , and  $t = 0.38$  mm are the Young modulus, Poisson ratio, and thickness of the silicon substrate, respectively;  $d$  ( $\sim 100$  nm) is the film thickness, and  $R_0$  and  $R$  are, respectively, the radii of curvature of the substrate before and after the film is deposited. The accuracy of the stress measurement is  $\sim 15\%$ . It is important to keep in mind that the intrinsic stress is a macroscopic property and represents the average biaxial internal pressure suffered by the matrix and thus transmitted to the implanted noble gases.

## III. RESULTS

### A. Noble-gas local environment (XANES/EXAFS)

Figure 1 shows the raw x-ray-absorption spectra of Ar implanted in the *a*-C matrix under several internal pressures. In a similar way, the x-ray-absorption spectra of Kr and Xe trapped in the *a*-C matrix as a function of the intrinsic stress

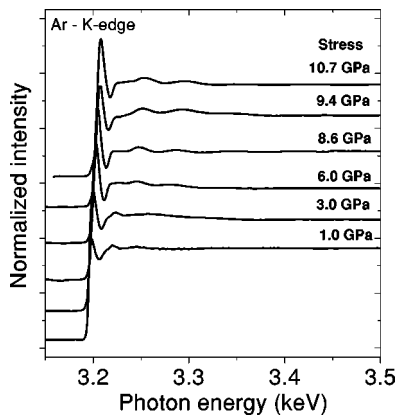


FIG. 1. Normalized  $K$  edge absorption spectra of Ar implanted in  $a$ -C films as a function of the intrinsic stress.

are depicted in Figs. 2 and 3. The evolution of the absorption spectra with increasing internal pressure indicates, for the three noble gases, a change in the local environment surrounding the NG atoms. Some fingerprints can be clearly observed. In the near-edge part of the spectra (XANES) ( $<50$  eV from edge) for all gases, there is a remarkable increase in the white line (first peak) as the internal stress increases. The white line is interpreted as an electronic transition from occupied core states to unoccupied states above the Fermi level. In other words, the white line reflects the unoccupied density of states.<sup>1-3</sup> Furthermore, the presence of the white line in the x-ray-absorption spectra of NGs is a characteristic feature of NGs in condensed phases. It is usually not observed in free noble-gas spectra. Note also that the Xe spectra (Fig. 3) present a second feature besides the white line peak. This second peak is of unknown origin and efforts to interpret it are currently under way. The analysis of the EXAFS spectra also discloses other interesting results. It can be observed in Figs. 1 and 3 that, as the internal pressure increases, not only does the white line intensity increase but also the EXAFS oscillations become more evident. These results provide evidence that a change in the NG environment takes place around the absorbing atom as the matrix pressure increases. Surprisingly, the analysis of the EXAFS signal shows that the first neighbor interatomic separation for both Ar and Xe, obtained from Fourier transform of the EX-

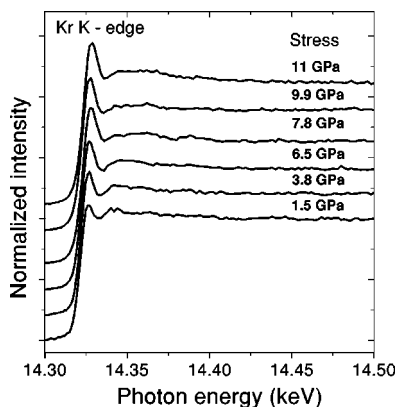


FIG. 2. Normalized  $K$  edge absorption spectra of Kr atoms implanted in  $a$ -C films as a function of the intrinsic stress.

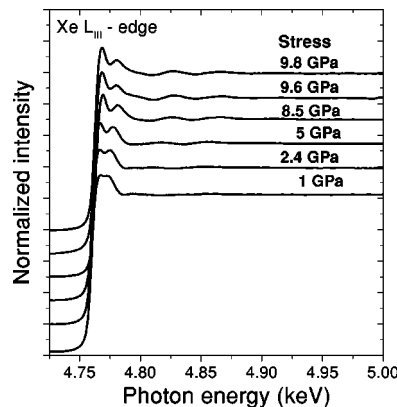


FIG. 3. Normalized  $L_{III}$ -edge absorption spectra of Xe atoms implanted in  $a$ -C films as a function of the intrinsic stress.

AFS signal, increases with pressure, see Figs. 4 and 5. This is an unexpected result, since one would expect a decrease of the interatomic distance with increasing pressure. In the case of Kr, the EXAFS oscillations are not so evident, thus no information concerning the interatomic distance could be drawn. For Ar (Xe), the first interatomic separation varies from 2.4 (2.9) Å to 2.9 (3.2) Å in the 1–11-GPa pressure range. A phase-shift correction of 0.4 Å for Ar and another of 0.3 Å for Xe was determined using the FEFF code.<sup>19</sup> As is further discussed, the evolution of the white line, observed in Figs. 1–3, as well as the increase in the first-neighbor distance (from EXAFS) support the fact that the matrix pressure is provoking an agglomeration process on the trapped NGs.

## B. NG electronic structure

The effect of the matrix pressure is not only restrained to promoting physical changes on the NGs, but also to simultaneously squeezing the outer valence wave function of the implanted NGs. The latter phenomenon can promote significant changes in the electronic structure (core-level energy) of the trapped NG atoms. Figure 6 depicts, under different internal pressures of the  $a$ -C matrix, the core-level energy changes suffered by all the NGs. It is to be noted that if one extrapolates the binding energy to zero pressure (which would be the equivalent for free noble gases) a difference of

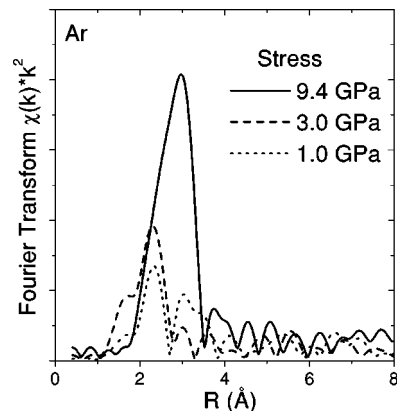


FIG. 4. Pseudoradial distribution function (RDF) obtained from the  $k^2$  weighted Fourier transform of the Ar EXAFS signal.

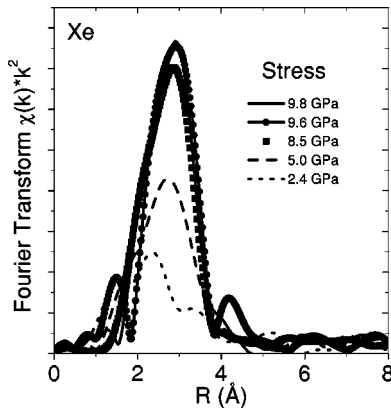


FIG. 5. Pseudo-RDF obtained from the  $k^2$  weighted Fourier transform of the Xe EXAFS signal.

6–7 eV is found because the binding energies of implanted gases (as in our case) are referenced to the Fermi level of the host matrix, as mentioned in Sec. II, whereas a “free” gas binding energy is referenced relative to the vacuum level. However, the original and important physical phenomenon demonstrated in Fig. 6 is the relative shift of the core-level energies as the pressure increases. There is a significant chemical binding-energy(BE) shift of about 0.9 eV to lower binding energies with increasing intrinsic stress. An approximately linear relationship is found between the BE and the internal pressure. In addition, the  $M_{4,5}$  nearest-neighbor Auger transitions (in kinetic energy) of Xe [see Fig. 6(a)] also show an even larger energy shift of about 1.7 eV. These results demonstrate the intrinsic relation between the electronic levels of the trapped NGs and the carbon matrix. A careful analysis is needed to understand a core electron energy shift of a nonbonded atom trapped in a matrix.

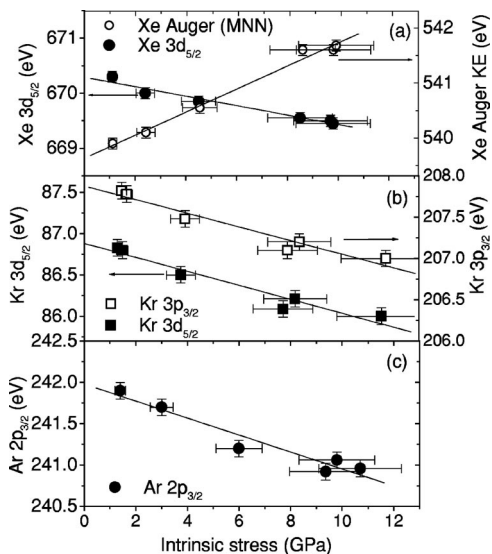


FIG. 6. Implanted noble-gas binding-energy shifts (relative to the Fermi level) as a function of the compressive stress of  $a$ -C films.

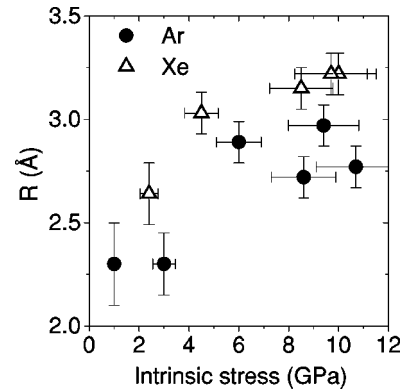


FIG. 7. Variation of the interatomic first-neighbor distance of implanted Ar and Xe atoms with the intrinsic stress of the  $a$ -C matrix.

#### IV. DISCUSSION

##### A. Noble-gas local environment (XANES/EXAFS)

In order to understand the increase in the white line intensity of NGs, we adopt the usual model in which this feature is a consequence of electronic transitions occurring from core states to unoccupied states above the Fermi level, that is, to a continuum of states. Noble gases interact through weak van der Waals interactions. Therefore, strong white lines are not observed in free NGs, and in some cases, such as those for Ar and Ne, only transitions to rydberg states have been seen.<sup>20,21,24</sup> On the other hand, strong white lines have been observed in Ne, Ar, and Kr clusters, in compounds such as KrF<sub>2</sub>, and in the solid state.<sup>1–3,20–22</sup> In addition, the white line has also been detected in Kr and Ar clusters implanted in Be,  $c$ -Si, and metals.<sup>6,10,23</sup> Then, the white line reflects, to a certain extent, the degree of interaction between the wave functions of NG atoms. It can be used to probe the presence of other NG atoms around the absorbing atom. Thus, the evolution of the white line observed in Figs. 1–3, is strong evidence that the matrix pressure is provoking some agglomeration process on the implanted NGs. For instance, Di Ciccio *et al.* observed a similar behavior in hydrostatic experiments on solid Kr.<sup>22</sup> In this work, the authors found that, as the external pressure increases, the Kr-Kr first-neighbor distance decreases (as expected) leading to an increased interaction between the NG outer valence wave functions. As a result, an increase of the white line intensity is observed. Another possible mechanism that could enhance the white line is a pressure-induced change of local coordination. We believe that, in our case, the white line increase is related to an increase of the interaction between NG neighbors via internal pressure and/or by a possible increase in the NG local coordination.

Figure 7 shows in detail the increase of the NG first-neighbor distance with increasing internal stress. The first-neighbor distance increase is the consequence of a local environment change induced by the matrix internal pressure. We can interpret this behavior as follows. First, when the internal pressure is low, the NGs are randomly diffused within the carbon matrix, so that only carbon atoms surround the implanted NG atoms. Thus, the NG x-ray-absorption spectra should be consistent with those of the gas phase.

Second, the increase of the internal pressure induces the NG atoms to get closer to each other, generating a change in NG local environment (from C to NG atoms). In other words, for low stress, the Ar (Xe) atoms are mainly “coordinated” to carbon (C) atoms from the lattice, which accounts for the obtained small interatomic distance. In fact, the Ar x-ray absorption for low stress ( $<3$  GPa) resembles that of free Ar atoms.<sup>24</sup> As the pressure increases, the Ar (Xe) atoms also start to “coordinate” with other Ar (Xe) atoms. As a consequence, the interatomic distance increases, reflecting this new environment. Due to the high EXAFS cross section of Ar (Xe) atoms and the small mass of carbon, the Ar (Xe) neighbors dominate the EXAFS signal, leading to a higher first-neighbor distance. It is also worth commenting upon the similarity between the clustered Ar x-ray spectra under high pressure ( $<6$  GPa) and those found in free Ar clusters and solids.<sup>2,24</sup> At high pressure the interatomic distance for Ar (2.9 Å) is comparable, but still smaller than that of Ar-Ar interatomic distance of highly compressed solid Ar.<sup>5</sup> This difference is assigned to some contribution of C atoms to the EXAFS signal, which also suggests that the cluster size is small. In fact, we could not observe the second and third shell peaks in the radial distribution functions (p-RDF) (Figs. 4 and 5) of Ar and Xe. These peaks are always present in solid NGs, or in large NG clusters.<sup>2,4</sup> Similar data for solid Xe is still lacking in the literature. However, it seems that the same behavior also holds for Xe. We also mention that the liquid-solid transition at room temperature is expected to be around 1.3 GPa for Ar,<sup>5</sup> around 1.15 GPa for Kr,<sup>20</sup> and about 0.8 GPa for Xe.<sup>25</sup> This indicates that the NG clusters in the carbon films presented here are in the solid phase. Summarizing, we observed a step-by-step NG clustering by controlling the internal pressure of the *a*-C host matrix. We propose that, during growth, the NGs permeate within the graphitic *a*-C network and are compressed against each other by other carbon atoms. Furthermore, since the carbon matrix is graphiticlike (90% *sp*<sup>2</sup>), it is likely that the NG atoms would be trapped between graphitic planes, thus forming two-dimensional(2D) clusters.

To provide support to the above interpretations, Merck molecular force field<sup>26</sup> (MMFF) calculations were performed on large graphitic clusters made up of two graphene sheets with fixed interplanar distances at the borders. The distance at the borders was allowed to assume values from from 3.6 (higher pressure) to 5.0 (lower pressure) Å. Argon atoms were randomly placed in between the graphene sheets, one by one, up to four atoms, allowing full geometrical relaxation except for the border interatomic distance. The clustering of Ar atoms in planar arrangements, see Fig. 8(a), was evident from these calculations when the “pressure,” namely, the constrained border distance, was varied. Curiously, Ar-Ar interatomic distance obtained from the high-pressure calculation values were about that experimentally obtained ( $\sim 2.9$  Å), and the cluster achieved a particular geometry [see Fig. 8(b)]. It suggests that the arrangement of carbon rings in the film controls the position of the NG atoms.

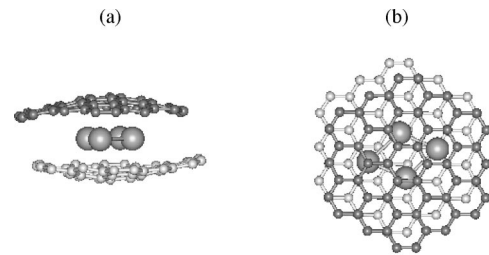


FIG. 8. Top and side views of molecular scheme showing the optimized 2D lozenge Ar cluster trapped between two graphene sheets.

### B. NG electronic structure

Similarly to the observation of clustering, the intrinsic relation between the matrix pressure and the BE shifts have not yet been reported. So far, some investigations of NGs implanted in matrices such as *c*-Ge, Al, Cu, and Au, (Refs. 27 and 28) have focused on the core-level binding-energy differences between implanted and free NGs. However, in Fig. 6, we observe a relative chemical shift depending on the pressure exerted by the *a*-C matrix only. It is also worth mentioning that the observed dependence of both BE and Auger peak positions on increasing compressive stress can be used as an interesting method for determining the stress of amorphous thin films. In other words, it is possible to determine the stress of a thin film by measuring the core-level energy position of the implanted gases. It is well known that deposition systems, such as ion-beam sputtering, rf sputtering, and glow discharge, are very common in industry and frequently use noble gases for thin-film preparation, as well as to sputter-clean surfaces or for depth profiling.<sup>29</sup> This implies that a low percentage of NGs is always implanted into the host structure. This proposal can be of significant interest for industrial applications. The main advantage of this method is the possibility of measuring the internal stress of very thin films (5–100 nm) which would be very difficult to determine using conventional techniques.

We can understand the changes observed in the core-levels in terms of two main contributions: First, a change in the initial-state energy (Koopman’s energy) at the NG core electron level owing to the compression by the host matrix of the outer valence wave function of the NG and second, a final-state extra-atomic relaxation, or screening process, provided by the valence electrons of the host. Previous experimental and theoretical work of NGs implanted in metals have suggested that the main contribution to the binding-energy difference, between implanted and free NGs, lies in the extra-atomic relaxation process. Thus, the change in the initial state due to the compression of the outer NG valence wave functions was considered to play a minor role in the overall BE shift.<sup>27,28</sup> Nevertheless, these investigations were performed in single “matrix” pressure conditions. In our case, we were able to vary the host matrix pressure by an order of magnitude and, as is demonstrated further on, it is clear that under certain circumstances the initial-state contribution cannot be completely disregarded.

### C. Theoretical calculations on core ionization energies

Electronic structure calculations were carried out to assess the problem and investigate the influence of the pressure on

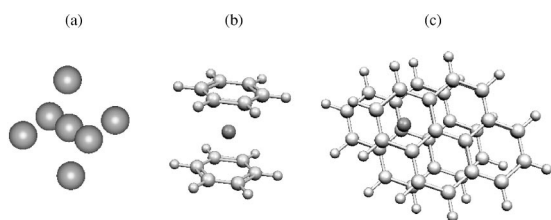


FIG. 9. (a) Seven-atom Ar cluster in octahedral symmetry with varying Ar-Ar distance; (b) one Ar atom in the center of a cluster comprising two benzene molecules in  $C_{6v}$  symmetry; (c) one Ar atom between two pyrene molecules at interplanar distances of 4.0 Å and 3.6 Å, where the aromatic molecules face each other as in graphite ( $C_s$  symmetry).

the core electron BE of noble gases. Argon has been chosen as the prototype noble gas. Ar-Ar and Ar-C interactions were investigated through the following model systems (Fig. 9): (i) a seven-atom Ar cluster in the octahedral symmetry with varying Ar-Ar distance; (ii) one Ar atom in the center of a cluster comprising two benzene molecules in  $C_{6v}$  symmetry, with a varying benzene interplanar distance; (iii) one Ar atom between two pyrene molecules at interplanar distances of 4.0 Å and 3.6 Å, where the aromatic molecules face each other as in graphite ( $C_s$  symmetry). In this structure the Ar atom is placed in the center of a six-membered ring, equidistant from all first-neighboring C atoms. The above choice of aromatic models to study Ar-C interaction is justified, since the  $\alpha$ -C matrix contains large amounts of  $sp^2$  carbon ( $\sim 90\%$ ). The molecular geometries of the isolated aromatic molecules were optimized using the (MMFF) method of the SPARTAN package.<sup>30</sup> Electronic structure calculations at the restricted Hartree-Fock (RHF) level, adopting the 6-31-G ( $p,d$ ) basis set, were performed using the GAMESS package.<sup>31</sup> For all clusters, the  $2p$  binding energy of the central Ar atom has been evaluated in two ways: first, by taking the associated one-electron orbital energy (Koopman's theorem) of the RHF spectrum as the initial-state contribution to the binding energy, and second, by calculating total-energy differences [the so-called self-consistent field results ( $\Delta$ SCF) method] between the neutral cluster and the one having the ionized core Ar atom. Therefore,  $\Delta$ SCF is the theoretical equivalent of the measured BE. The pressure effect is simulated by manipulating of the Ar-Ar or Ar-C distance without further geometrical relaxation.

Figure 10 displays the theoretical calculations of the total energy ( $\Delta$ SCF), the initial state (Koopman's theorem), and the relaxation contributions to the binding-energy shift of the Ar  $2p$  core-level from  $Ar_7$  cluster as a function of pressure. The conversion from interatomic distance to pressure was made using the x-ray data on solid argon from Ref. 5. The experimental BE shift of the Ar  $2p$  core-level for implanted Ar is also shown for comparison. There are at least two important findings of the calculations above: (i) the core-level BE of Ar in the  $Ar_7$  cluster is dependent on the pressure; (ii) both the initial state and relaxation contribute significantly to the BE shift.

The BE shift for the  $Ar_7$  cluster is smaller than that experimentally obtained for implanted Ar in the  $\alpha$ -C matrix, Fig. 10. The reason for this difference can be attributed to the

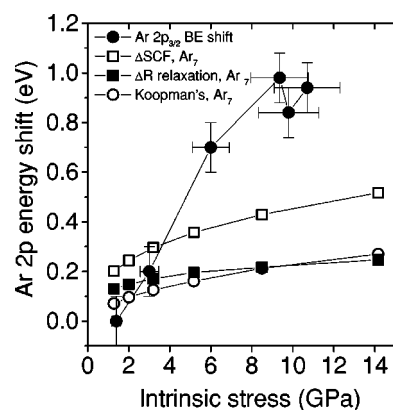


FIG. 10. Experimental BE shift of implanted Ar  $2p$ , and calculated  $\Delta$ SCF, relaxation energy, and Koopman's energy for the  $Ar_7$  clusters as a function of the pressure.

fact that the  $Ar_7$  cluster is a less polarizable system and it does not have the surrounding atoms of the carbon matrix and its valence electrons. This effect can be observed in a similar calculation performed on an Ar atom trapped by two benzene or two pyrene molecules, see Table I. It can be readily noticed that the total energy is very sensitive to the pressure (via interatomic distance) as well as to the environment. Thus, the presence of the carbon matrix may be responsible for the larger BE shift determined experimentally. Another possibility may be related to an increase in the cluster size as the pressure increases. In fact, previous studies of free Ar clusters have demonstrated that the core-level BE depends on the cluster size as well.<sup>32</sup> However, the EXAFS analysis indicates that our cluster sizes might be small. Thus, one expects a small contribution related to the variation in the cluster size.

The calculations also predict that the contribution from the initial state is comparable to the relaxation term. Experimentally, the relaxation energy ( $DR$ ) can be determined by using the Auger parameter as proposed by Wagner (for a recent review, see, for instance, Refs. 33 and 34). Briefly, the Auger parameter ( $\alpha$ ) is defined as the difference between the energies of the core and Auger electrons ( $\alpha = K + E$ , where  $K$  is the kinetic energy of the Auger electron and  $E$  is the binding energy of the core electron). Assuming that all core-levels of the probed atom shift by the same amount of energy, which is valid for Kr  $3p$  and Kr  $3d$ , and also for Xe  $3d$  and Xe  $4d$  (not shown), the Auger parameter shift ( $\Delta\alpha$ ) between two chemical states can be written as  $\Delta\alpha = 2\Delta R$ , where  $\Delta R$  is the corresponding final-state extra-atomic relax-

TABLE I. Ar  $2p$  binding energies from RHF calculations for Ar in benzene ( $C_6H_6$ ) and pyrene ( $C_{16}H_{10}$ ) dimers: Koopman's ionization energy ( $-\epsilon_{2p}$ ) and relaxed binding energy ( $\Delta$ SCF), all in eV, as a function of Ar-C distance;  $R$ , is in angstroms.

	Ar in ( $C_6H_6$ ) <sub>2</sub>				Ar in ( $C_{16}H_{10}$ ) <sub>2</sub>	
$R$ (Å)	2.20	2.28	2.36	2.44	2.05	2.25
$-\epsilon_{2p}$	256.5	256.8	257.2	257.5	258.2	258.2
$\Delta$ SCF	245.9	246.4	246.8	247.2	246.9	247.2

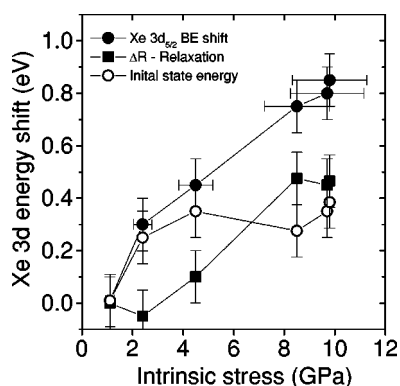


FIG. 11. Experimental Xe 3d BE shift,  $\Delta R$  relaxation energy (from Auger parameter), and obtained initial-state energy as a function of the internal stress.

ation energy.<sup>33,34</sup> Then, by combining the core-level and Auger energy positions we can experimentally extract the  $\Delta R$  relaxation energy. Subsequently, by subtracting  $\Delta R$  from the measured BE shift, one can estimate the initial-state (Koopman's) contribution ( $BE = -\epsilon - R$ ). Unfortunately, we were only able to measure the Auger peak for implanted Xe. Since the total BE shifts of all the NGs are similar, we expect the qualitative behavior for the initial-state and relaxation terms to hold for the other NGs. Figure 11 depicts, for Xe, the total BE shifts, the relaxation energy, and the initial-state contributions as a function of the internal pressure of the *a*-C matrix (the energy value for the lowest stressed film was taken as the reference). It can be inferred from Fig. 11 that, at low stress, the BE shift is dominated by the change in the initial state owing to the compression of the outer valence wave functions of the NG. Therefore, in this case, the relaxation energy contribution is not significant. On the other hand, at high pressure the initial-state component becomes constant and the BE shift is augmented by the increase in the relaxation energy. It is interesting to note that at higher pressures ( $>4$  GPa) both initial-state and relaxation energies contribute almost the same to the BE shift, a result similar to that theoretically found for the Ar<sub>7</sub> clusters, see Fig. 10. In addition, the calculated data presented in Table I, for an Ar atom surrounded by aromatic molecules, clearly demonstrate that for all interatomic distances both the initial-state and relaxation terms contribute to the shift in the Ar 2*p* BE. Nevertheless, the contribution of each term depends also on the local Ar environment. For instance, taking the interatomic distances from 2.20 Å to 2.36 Å, in the benzene dimer, one has a 0.9-eV total BE shift with 0.7 eV coming from the initial state. On the other hand, certain geometrical arrangements of the noble gases in the matrix might force a "binding" of Ar to C at high pressure, for which the host

relaxation becomes more important than the initial state, as seen in the result of Ar clustered in a pyrene dimer.

## V. CONCLUSIONS

In summary, we presented in this work an approach for studying noble gases under pressure. By intentionally controlling the internal biaxial stress of the *a*-C matrix, we were able to trap noble gases under different internal pressures ranging from 1 to 11 GPa. From the analysis of the EXAFS oscillations, we observed that there is an increase of the NG first-neighbor distance with increasing internal stress. This increase is attributed to a change in the local environment surrounding the NG atoms. At low pressure only carbon atoms surround NG atoms. However, as the internal pressure increases an induced agglomeration process takes place, and NG atoms starts to "coordinate" with other NG atoms. This explanation is supported by the increase of the white line intensity (XANES), which evidences an increasing interaction between noble gases atoms with increasing internal stress. Molecular mechanics calculations were performed, providing support to the model of clustering of noble-gas atoms (Ar) between graphitic molecules under external pressure. Based on these results, we propose the formation of 2D NG clusters squeezed by graphitelike planes of the *a*-C matrix. The internal pressure also affects the outer electron valence wave functions of the implanted noble gases and promotes a change in their core electronic levels. A shift to lower binding energy ( $\sim 1$  eV) is observed as the internal stress increases. Auger and XPS measurements were used to separate the contribution from the initial- and final-state (relaxation) energies due to the increased pressure. From this analysis, we verified that both initial-state and relaxation terms contribute to the shift in the core-level energy. These experimental results are supported by *ab initio* electronic structure calculations performed in Ar<sub>7</sub> clusters and one Ar atom trapped between aromatic molecules. External pressure was shown to affect both the initial-state electronic structure of the noble-gas atom and the interaction of NGs with the host matrix. Since as the noble gases are less polarizable than the *sp*<sup>2</sup> carbon environment, the final-state contribution to the shift in binding energy was shown to come mostly from the host electronic relaxation upon core ionization of the NG.

## ACKNOWLEDGMENTS

This work has been partially performed at the LNLS - National Synchrotron Light Laboratory, Brazil and was supported by CNPq and FAPESP. The authors are grateful to G. Kleimann for stimulating discussions and A. Ramos for the EFFF analysis.

\*Corresponding author. Email address: rgl26@eng.cam.ac.uk

<sup>1</sup>F. Federmann, O. Bjorneholm, A. Beutler, and T. Moller, Phys. Rev. Lett. **73**, 1549 (1994).

<sup>2</sup>S. Kakar *et al.*, Phys. Rev. Lett. **78**, 1675 (1997).

<sup>3</sup>A. Knop, B. Wassermann, and E. Ruhl, Phys. Rev. Lett. **80**, 2302 (1998).

<sup>4</sup>A.B. Belonoshko, R. Ahuja, and B. Johansson, Phys. Rev. Lett. **87**, 165505 (2001).

<sup>5</sup>L.W. Finger *et al.*, Appl. Phys. Lett. **39**, 892 (1981).

<sup>6</sup>G. Faraci, A.R. Pennisi, A. Terrasi, and S. Mobilio, Phys. Rev. B **43**, 9962 (1991).

<sup>7</sup>H. Cynn *et al.*, Phys. Rev. Lett. **86**, 4552 (2001).

- <sup>8</sup>S.E. Donnelly and C.J. Rossouw, *Science* **230**, 1272 (1985).
- <sup>9</sup>A. von Feld *et al.*, *Phys. Rev. Lett.* **53**, 922 (1995).
- <sup>10</sup>G. Faraci, A.R. Pennisi, and J.L. Hazemann, *Phys. Rev. B* **56**, 12 553 (1997).
- <sup>11</sup>R.C. Birtcher *et al.*, *Phys. Rev. Lett.* **83**, 1617 (1999).
- <sup>12</sup>R.G. Lacerda, P. Hammer, C.M. Lepienski, F. Alvarez, and F.C. Marques, *J. Vac. Sci. Technol. A* **19**, 971 (2001).
- <sup>13</sup>C.H. Poa, R.G. Lacerda, D.C. Cox, S.R.P. Silva, and F.C. Marques, *Appl. Phys. Lett.* **81**, 853 (2002).
- <sup>14</sup>H. Tolentino *et al.*, *J. Synchrotron Radiat.* **5**, 521 (1999).
- <sup>15</sup>M. Abbate *et al.*, *J. Synchrotron Radiat.* **6**, 964 (1999).
- <sup>16</sup>M.M. de Lima, Jr., R.G. Lacerda, J. Vilcarromero, and F.C. Marques, *J. Appl. Phys.* **86**, 4936 (1999).
- <sup>17</sup>G.C. Stoney, *Proc. R. Soc. London, Ser. A* **32**, 172 (1909).
- <sup>18</sup>R.W. Hoffman, *Physics of Non-Metallic Thin Films*, (Plenum, New York, 1970) Vol. B-14.
- <sup>19</sup>Computer code FEFF; S.I. Zabinsky *et al.*, *Phys. Rev. B* **52**, 2995 (1995).
- <sup>20</sup>H.C. Schmelz *et al.*, *Physica B* **208**, 519 (1995).
- <sup>21</sup>F.W. Kutzler *et al.*, *Solid State Commun.* **46**, 803 (1983).
- <sup>22</sup>A. Di Ciccio, A. Filliponi, J.P. Itie, and P. Polian, *Phys. Rev. B* **54**, 9086 (1996).
- <sup>23</sup>G. Faraci, A.R. Pennisi, A. Terrasi, and S. Mobilio, *Phys. Rev. B* **38**, 13 468 (1988).
- <sup>24</sup>E. Ruhl *et al.*, *J. Chem. Phys.* **98**, 6820 (1993).
- <sup>25</sup>A.N. Zisman, I.V. Aleksandrov, and S.M. Stishov, *Phys. Rev. Lett.* **32**, 484 (1985).
- <sup>26</sup>T.A. Halgren, *J. Comput. Chem.* **17**, 490 (1996).
- <sup>27</sup>P.H. Citrin and D.R. Hamann, *Phys. Rev. B* **10**, 4948 (1976).
- <sup>28</sup>B.J. Wacławski, J.W. Gadzuk, and J.F. Herbst, *Phys. Rev. Lett.* **41**, 583 (1978).
- <sup>29</sup>E.L. Fleicher and M G. Norton, *Heterog. Chem. Rev.* **3**, 171 (1996).
- <sup>30</sup>Computer code SPARTAN package version 5.0 (Wavefunction Inc., Irvine, California).
- <sup>31</sup>M.W. Schmidt *et al.*, *J. Comput. Chem.* **14**, 1347 (1993).
- <sup>32</sup>O. Bjorneholm, F. Federmann, F. Fossing, and T. Moller, *Phys. Rev. Lett.* **74**, 3017 (1995).
- <sup>33</sup>C.D. Wagner, *Faraday Discuss. Chem. Soc.* **60**, 291 (1975).
- <sup>34</sup>G. Moretti, *J. Electron Spectrosc. Relat. Phenom.* **95**, 95 (1998).